QM/MM modelling of oleamide hydrolysis in fatty acid amide hydrolase (FAAH) reveals a new mechanism of nucleophile activation†

Alessio Lodola,[a] Marco Mor,[a] Johannes C. Hermann,[b] Giorgio Tarzia,[c] Daniele Piomelli[d] and Adrian J. Mulholland*[b]

Received (in Cambridge, UK) 17th March 2005, Accepted 8th June 2005
First published as an Advance Article on the web 11th July 2005
DOI: 10.1039/b503887a

Fatty acid amide hydrolase (FAAH), a promising target for the treatment of several central and peripheral nervous system disorders, such as anxiety, pain and hypertension, has an unusual catalytic site, and its mechanism has been uncertain; hybrid quantum mechanics/molecular mechanics (QM/MM) calculations reveal a new mechanism of nucleophile activation (involving a Lys–Ser–Ser catalytic triad), with potentially crucial insights for the design of potent and selective inhibitors.

Fatty acid amide hydrolase (FAAH) is a member of the amidase signature (AS) family that plays a major role in the inactivation of neuromodulatory lipid amides such as the endogenous cannabinoid anandamide and the sleep-inducing substance oleamide.[1] Studies of FAAH-deficient mice have confirmed that this enzyme is a key regulator of fatty acid amide signalling *in vivo*.[2] A new class of carbamic acid aryl esters[3,4] shows profound *in vivo* inhibition of FAAH activity after systemic administration in rodents, suggesting this enzyme as an attractive target for the treatment of anxiety.[5] Further investigations have demonstrated the potential of FAAH inhibitors in the treatment of pain[6] and hypertension.[7] In this light, understanding of the catalytic mechanism of FAAH may assist in the design of new inhibitors (*e.g.* 'mechanism-based'), which could provide the potency and selectivity required for clinical applications. Here, we have applied a well-tested quantum mechanics/molecular mechanics (QM/MM)[8] approach to analyse, at the atomic level, the first step of the acylation reaction between FAAH and the substrate oleamide. High-level QM corrections have been applied, and the results are consistent with experimental data. The calculations reveal a novel mechanism. The proposed pathway, modelled here for the first time, shows that Lys142 and Ser217 cooperate to activate the nucleophilic Ser241. The calculations also identify key catalytic interactions at the active site. This new mechanistic insight should be useful in inhibitor design.

The recent solution of the crystal structure of FAAH covalently bound to methyl arachidonyl phosphonate (MAP),[9] and enzymological studies of mutants,[10] indicate that the catalytic machinery of this enzyme is a serine–serine–lysine catalytic triad, in contrast to the classical serine–histidine–aspartate triad found in most serine hydrolases. This unusual triad is assumed to be responsible for FAAH's ability to hydrolyse amides and esters at equivalent rates, by a mechanism in which acylation is rate-limiting.[11] The pH–activity profile suggests that Lys142 may act as a general base.[11] However, its role in the activation of the nucleophilic Ser241, the contribution of Ser217, and the precise mechanism of this unusual reaction remain unclear. With this in mind, we have modelled the mechanism of the crucial first steps of the acylation reaction by a hybrid (QM/MM) approach, which has been shown to provide detailed and useful mechanistic insights for enzyme reactions.[12–14] In combination, we have used high level hybrid density-functional theory (DFT) calculations for a reliable description of the reaction energetics. This approach has recently been successfully applied to model the mechanism of a Class A β-lactamase.[15]

A molecular model of the functional subunit of FAAH, in complex with the substrate oleamide (9*Z*-octadecenamide), was prepared starting from the FAAH–MAP crystal structure.[9] CHARMM (version 27b2) was used for all calculations.[16] The MAP inhibitor was transformed into oleamide by changing atom and bond types (using standard CHARMM27 lipid parameters[17]) and optimizing the geometry by MM. The minimized molecule was superimposed on (and replaced) the MAP inhibitor in the enzyme binding site. The resulting oleamide complex was solvated by a 25 Å radius sphere of TIP3P water molecules and equilibrated by 280 ps of CHARMM MM molecular dynamics (MD),[17] following the procedure described in ref. 13. The structure was minimized (MM) to an energy gradient of 0.01 kcal mol^{-1} $Å^{-1}$ with the ABNR method,[16] before the QM/MM calculations. In the QM/MM modelling, the methylamine group of Lys142, the side chains of Ser217 and Ser241 and the butanamide fragment of oleamide were treated at the PM3[18] quantum chemical level, while the other atoms (7490) were treated at the MM level with the CHARMM all-atom force field employing CHARMM22 parameters for the protein and CHARMM27 parameters for the lipid.[17] The covalent bonds, which cross the boundary between the QM and MM regions, were treated by introducing four 'HQ' link atoms,[8] which are included in the QM system (34 atoms in total). This well-tested QM/MM method includes bonded and non-bonded interactions between the QM and MM systems. Van der Waals and bonded interactions are represented by molecular mechanics terms, with standard CHARMM22 and CHARMM27 parameters for the QM atoms.† Electrostatic interactions are treated by including the MM atomic charges (as atomic 'cores') in

[a]*Dipartimento Farmaceutico, Università degli Studi di Parma, 43100, Parma, Italy*
[b]*School of Chemistry, University of Bristol, Bristol, UK BS8 1TS. E-mail: Adrian.Mulholland@bristol.ac.uk*
[c]*Istituto di Chimica Farmaceutica e Tossicologica, Università degli Studi di Urbino "Carlo Bo", 61029, Urbino, Italy*
[d]*Department of Pharmacology, University of California, 92697-4625, Irvine, California, USA*
† Electronic supplementary information (ESI) available: van der Waals parameters for the QM atoms. See http://dx.doi.org/10.1039/b503887a

the Hamiltonian for the QM system, thus including the vital effects of the protein environment on the reaction.[8] In all the simulations, a nonbonded cutoff of 12 Å was applied using a group-based switching function to scale the electrostatic interactions smoothly down over 8–12 Å. Atoms further than 14 Å from the Ser241 hydroxyl oxygen were fixed. Apart from these boundary restraints, all the other atoms were free to move during the calculations.

The adiabatic mapping approach, which has been shown to perform well for similar enzyme reactions,[14,15,19] was used to calculate potential energy surfaces (PESs), generating models of the transition states and intermediates. The PES was explored by selecting two reaction coordinates (R_x and R_y) to represent the key steps of the acylation process (see Fig. 1C), *i.e.* deprotonation of Ser217 by (neutral) Lys142, proton transfer from Ser241 to Ser217, and nucleophilic attack on the carbonyl moiety of oleamide by Ser241, eventually leading to the formation of the tetrahedral intermediate, TI (**4**). R_x was defined as the difference of three interatomic distances ($R_x = d$[O1, H1] − d[O2, H1] − d[O1, C]), including proton abstraction from Ser241 by Ser217 and the nucleophilic attack by Ser241. R_y, defined as $R_y = d$[O2, H2] − d[N, H2], describes the proton transfer between Ser217 and Lys142. The use of two coordinates here ensures that Lys142 is not forced to take part in the reaction. R_x and R_y were increased respectively in steps of 0.2 and 0.1 Å with harmonic restraints of 5000 kcal mol^{-1} Å^{-2}. Geometry optimization of the structures was performed at each point to an energy gradient of 0.01 kcal mol^{-1} Å^{-1}. The energy was then computed by a single point calculation, removing the energy contributions due to reaction coordinate restraints. The complex coordinate R_x forces the reaction to involve proton transfer between Ser217 and Ser241. The importance of this transfer is supported by mutagenesis experiments. The stepwise increase in this reaction coordinate was freely distributed among the three distances during energy minimization, with an additional constraint that the distance d[C1,O1] could only decrease to ensure the overall progress of the reaction. Other reaction coordinates were also tested, but only the combination described here was found to drive the system from the reactant to the product along an energetically and structurally reasonable pathway. A similar approach was used for a Class A β-lactamase.[14,15] Moreover, different snapshots from the MD simulation were taken as starting points, and gave similar pathways. The surface and geometries presented here can therefore be regarded as being representative of the reaction.

The PM3-CHARMM PES (Fig. 1A) shows four minima: 1) the Michaelis (substrate) complex; 2) Lys142 protonated and Ser217 as the alcoholate ion; 3) Ser217 in the neutral form and Ser241 deprotonated; 4) the tetrahedral intermediate (TI), in which Ser241 is covalently bound to oleamide. These approximate stationary points are connected by three saddle points (transition state structures). The whole process can thus be described as follows (Fig. 1C): neutral Lys142 initiates reaction by accepting a proton from Ser217, leading to the formation of **2**. Ser217 deprotonates Ser241 to form the nucleophilic Ser241 anion (**3**). The total barrier, 36 kcal mol^{-1} (relative to the Michaelis complex) is overestimated by the semiempirical PM3 method (see below). The transient configuration (**3**) is stabilized by Ser217, by interaction of both its side chain hydroxyl and backbone NH with the charged oxygen of Ser241. This network of hydrogen bonds is close to an unusual *cis* peptide bond, between Ser217 and Gly216, which has been proposed to be essential for catalysis in other enzymes belonging to the AS family.[20] The subsequent nucleophilic attack produces **4** with effectively no barrier, indicating that TI formation and Ser241 deprotonation are concerted.

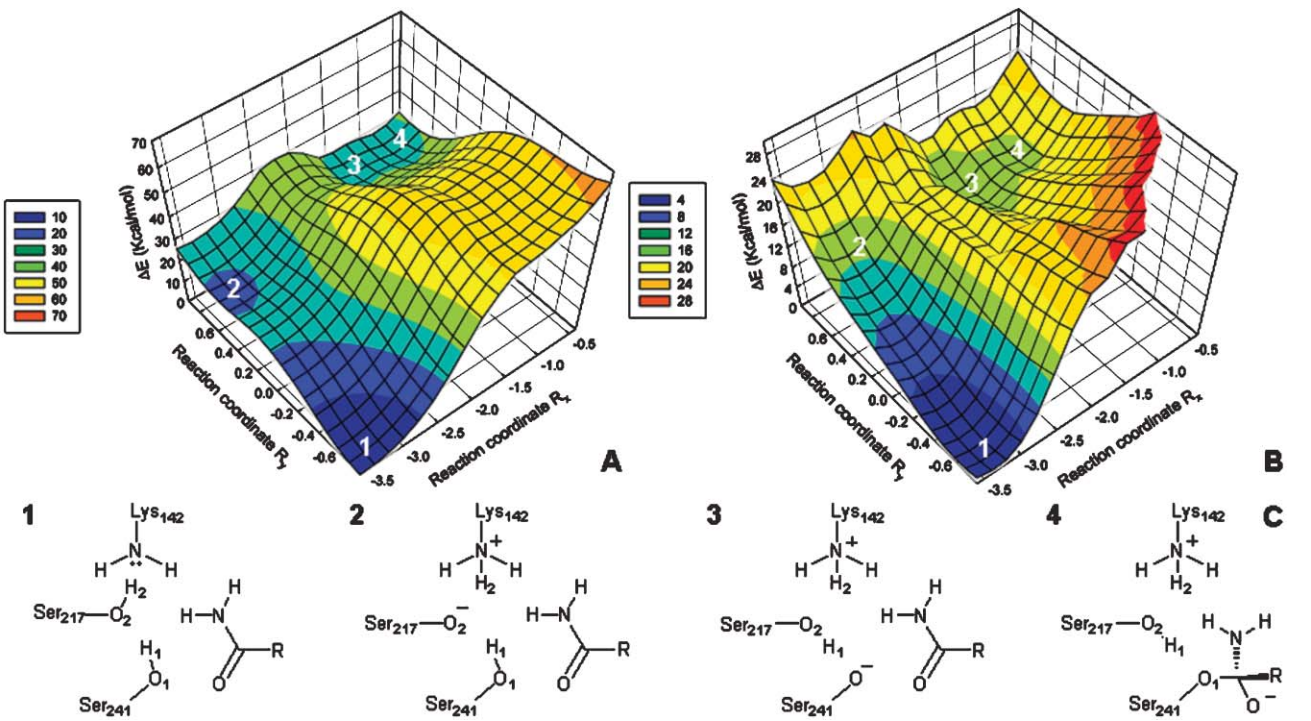

Fig. 1 (A) PM3/CHARMM and (B) B3LYP/6-31+G(d)//PM3-CHARMM potential energy surfaces of the first step of acylation in FAAH. (C) **1**, **2**, **3** and **4** are significant configurations along the reaction pathway. **4** is the tetrahedral intermediate (TI).

Semiempirical methods, such as PM3, often overestimate barriers,[12] so higher level calculations (B3LYP/6-31+G(d)) were used to correct the reaction energies. Similar approaches have been found to be important in modelling other enzymes.[15,21,22] The QM atoms of every structure (306 points per surface) were isolated and single point energy calculations were performed at the PM3 and B3LYP/6-31G+(d)[23] levels, respectively. The corrected PES was obtained by subtracting the PM3 energy of the isolated QM region from the total QM/MM energy, and adding the B3LYP energy. This gives a surface with the energetics of the reaction described at a reliable, high level (relatively insensitive to geometry), while also including the essential effects of the protein environment on the reaction.[15] The resulting QM/MM surface, denoted by B3LYP/6-31+G(d)//PM3-CHARMM (Fig. 1B), shows only three minima, in somewhat different positions from the lower-level PES (Fig. 1A). The geometry corresponding to configuration **2** is not a stationary point, indicating that the two proton transfers, leading to the nucleophilic Ser241 alcoholate ion, are concerted. The calculated barrier at the higher level (18 kcal mol^{-1}) is close to the experimentally deduced activation barrier of $\sim$16 kcal mol^{-1}.[10] The structure of the transition state (the highest energy point along the minimum energy path), and of neighbouring species, shows a proton being transferred from Ser241 to Ser217, *i.e.* the TS corresponds to activation of Ser241. A range of different geometries with similar energies can be considered possible TS structures along the 'seam' dividing **1** and **3**. Although the predicted TS involves proton transfer rather than nucleophilic attack, the absence of a significant barrier between **3** and **4** indicates that Ser241 activation and nucleophilic attack are effectively concerted. The tetrahedral intermediate is less stable than the Michaelis complex by 14 kcal mol^{-1}, indicating its transient character. The calculations show, however, that the TI is greatly stabilized by the enzyme, in particular by its 'oxyanion hole'. Similar stabilization mechanisms have been found for other enzymes specializing in amide bond cleavage, *e.g.* β-lactamases.[15] In FAAH, this active site feature is composed of four consecutive residues (Ile238, Gly239, Gly240 and Ser241) arranged in a hairpin-like loop. The backbone NH groups of all these residues donate hydrogen bonds to the oxygen of oleamide. As the reaction proceeds, these hydrogen bonds become stronger, as negative charge increases on this oxygen atom. The increase in strength of the hydrogen bonds is reflected by their shortening during the reaction. The stabilization by the enzyme reaches a maximum for the tetrahedral intermediate. The active site is well organized to achieve this stabilization, and so to catalyse the reaction effectively. Little structural change of the protein is observed along the reaction pathway.

The proposed mechanism, modelled here for the first time, shows that Lys142 and *cis*-Ser217 have a direct role in the activation of Ser241, in agreement with kinetic labelling experiments employing the highly reactive fluorophosphonate-tetramethyl rhodamine.[10] The greater reduction of Ser241 labelling rate in the K142A/S217A double mutant, compared to the K142A and S217A single mutants, suggests that Lys142 and Ser217 cooperate to deprotonate Ser241, as indicated by our calculations. Our results also concur with solvent deuterium isotope effects for oleamide hydrolysis,[11] which indicate that a proton transfer is involved in the rate-limiting step of the reaction. The pathway proposed here is structurally and energetically reasonable. It elucidates the roles of all the key residues, including Ser217. The mechanism found here provides new and detailed insight into the unusual catalytic machinery of FAAH that will be useful in understanding its biological function, and in ongoing inhibitor design.

AJM thanks BBSRC, EPSRC, The Royal Society (with JCH) and the IBM High Performance Computing Life Sciences Outreach Programme for support.

Notes and references

1 D. Piomelli, *Nat. Rev. Neurosci.*, 2003, **4**, 873–884.
2 B. F. Cravatt and A. H. Lichtman, *Curr. Opin. Chem. Biol.*, 2003, **7**, 469–475.
3 G. Tarzia, A. Duranti, A. Tontini, G. Piersanti, M. Mor, S. Rivara, P. V. Plazzi, C. Park, S. Kathuria and D. Piomelli, *J. Med. Chem.*, 2003, **46**, 2352–2360.
4 M. Mor, S. Rivara, A. Lodola, P. V. Plazzi, G. Tarzia, A. Duranti, A. Tontini, G. Piersanti, S. Kathuria and D. Piomelli, *J. Med. Chem.*, 2004, **47**, 4998–5008.
5 S. Kathuria, S. Gaetani, D. Fegley, F. Valino, A. Duranti, A. Tontini, M. Mor, G. Tarzia, G. La Rana, A. Calignano, A. Giustino, M. Tattoli, M. Palmery, V. Cuomo and D. Piomelli, *Nat. Med.*, 2003, **9**, 76–81.
6 A. H. Litchtman, D. Leung, C. C. Shelton, A. Saghatelian, C. Hardouin, D. L. Boger and B. F. Cravatt, *J. Pharmacol. Exp. Ther.*, 2004, **311**, 441–448.
7 S. Bátkai, P. Pacher, D. Osei-Hyiaman, S. Radaeva, J. Liu, J. Harvey-White, L. Offertáler, K. Mackie, M. A. Rudd, R. D. Bukoski and G. Kunos, *Circulation*, 2004, **110**, 1996–2002.
8 M. J. Field, P. A. Bash and M. Karplus, *J. Comput. Chem.*, 1990, **11**, 700–733.
9 M. H. Bracey, M. A. Hanson, K. R. Masuda, R. C. Stevens and B. F. Cravatt, *Science*, 2002, **298**, 1793–1796.
10 M. K. McKinney and B. F. Cravatt, *J. Biol. Chem.*, 2003, **278**, 37393–37399.
11 M. P. Patricelli and B. F. Cravatt, *J. Biol. Chem.*, 2000, **275**, 19177–19184.
12 A. J. Mulholland, P. D. Lyne and M. Karplus, *J. Am. Chem. Soc.*, 2000, **122**, 534–535.
13 L. Ridder, I. M. C. M. Rietjens, J. Vervoort and A. J. Mulholland, *J. Am. Chem. Soc.*, 2002, **124**, 9926–9936.
14 J. C. Hermann, L. Ridder, A. J. Mulholland and H. D. Höltje, *J. Am. Chem. Soc.*, 2003, **125**, 9590–9591.
15 J. C. Hermann, C. Hensen, L. Ridder, A. J. Mulholland and H. D. Höltje, *J. Am. Chem. Soc.*, 2005, **127**, 4454–4465.
16 B. R. Brooks, R. E. Bruccoleri, B. D. Olafson, D. J. States, S. Swaminathan and M. Karplus, *J. Comput. Chem.*, 1983, **4**, 187–217; see www.charmm.org.
17 A. D. MacKerell, Jr., D. Bashford, M. Bellott, R. L. Dunbrack, Jr., J. D. Evanseck, M. J. Field, S. Fischer, J. Gao, H. Guo, S. Ha, D. Joseph-McCarthy, L. Kuchnir, K. Kuczera, F. T. K. Lau, C. Mattos, S. Michnick, T. Ngo, D. T. Nguyen, B. Prodhom, W. E. Reiher, III, B. Roux, M. Schlenkrich, J. C. Smith, R. Stote, J. Straub, M. Watanabe, J. Wiórkiewicz-Kuczera, D. Yin and M. Karplus, *J. Phys. Chem. B*, 1998, **102**, 3586–3616.
18 J. J. P. Stewart, *J. Comput. Chem.*, 1989, **10**, 221–264.
19 L. Ridder, A. J. Mulholland, I. M. C. M. Rietjens and J. Vervoort, *J. Am. Chem. Soc.*, 2000, **122**, 8728–8738.
20 S. Shin, Y. S. Yun, H. M. Koo, Y. S. Kim, K. Y. Choi and B. H. Oh, *J. Biol. Chem.*, 2003, **278**, 24937–24943.
21 K. E. Ranaghan, L. Ridder, B. Szefczyk, W. A. Sokalski, J. C. Hermann and A. J. Mulholland, *Org. Biomol. Chem.*, 2004, **2**, 968–980.
22 L. Ridder, J. N. Harvey, I. M. C. M. Rietjens, J. Vervoort and A. J. Mulholland, *J. Phys. Chem. B*, 2003, **107**, 2118–2126.
23 *Jaguar 4.2*, Schrödinger, Inc., Portland, OR, 1991–2000.